



ELSEVIER

Catalysis Today 42 (1998) 283–295

---

---

**C** TODAY  
CATALYSIS  
TODAY

---

---

## Propane ammoxidation to acrylonitrile over a tin-based mixed-oxide catalyst

S. Albonetti<sup>a</sup>, G. Blanchard<sup>b</sup>, P. Burattin<sup>b</sup>, F. Cavani<sup>a,\*</sup>, S. Masetti<sup>a</sup>, F. Trifirò<sup>a</sup>

<sup>a</sup>*Department of Industrial Chemistry and Materials, University of Bologna, V.le Risorgimento 4, 40136 Bologna, Italy*

<sup>b</sup>*Rhone Poulenc Chimie, Rue De La Haie Coq 52, 93308 Aubervilliers, France*

---

### Abstract

The catalytic properties of a Sn/V/Sb mixed oxide for propane ammoxidation to acrylonitrile are studied in this paper. First, preparing the sample with a coprecipitation method from an ethanolic phase, the amounts of antimony and vanadium were changed in order to optimize the relative atomic ratio of the ternary catalyst. The results obtained indicate that vanadium is responsible for the paraffin activation and antimony for the insertion of nitrogen in the molecule (it can be considered as an acrylonitrile selectivity modulator). Other samples, with the optimized atomic ratio, were also prepared using a similar coprecipitation technique (but by dissolving the starting materials with iso-butanol or water instead of ethanol), or by solid state reaction between oxide and tin hydroxide. The sample prepared using ethanol shows the best catalytic performance. This solvent makes the partial alkoxides quite stable in solution and brings about better coprecipitation with a more intimate mixture of tin, antimony and vanadium. Finally, the thermal transformation of the precursor of this sample was followed during calcination, both in air and in nitrogen with several characterization techniques. The thermal treatment in air at 700°C leads to the best catalytic performance, i.e., good activity and high selectivity. © 1998 Elsevier Science B.V. All rights reserved.

**Keywords:** Ammoxidation of propane; Acrylonitrile; Rutile catalysts; Vanadium; Tin; Antimony mixed oxides

---

### 1. Introduction

Acrylonitrile (ACN) is being produced at present by the ammoxidation of propene on catalysts made of promoted Fe–Bi–Mo–O (SOHIO) or promoted Fe–Sb–O (Nitto). Nevertheless, in recent years some companies have decided to invest in research on the ammoxidation of propane [1].

One of the more interesting catalytic systems for the direct ammoxidation of the paraffin is Sb/V/O [2–7].

The synthesis of these catalysts is usually made by solid state reaction between  $V_2O_5$  and  $Sb_2O_4$  at 700°C or by reaction between  $NH_4VO_3$  and  $Sb_2O_3$ . Mossbauer analysis shows that antimony is mainly in its pentavalent state, so a large amount of vanadium is reduced, with the formation of  $V^{III}Sb^VO_4$  and the possible presence of  $V^{IV}$  in substitutional or interstitial solid solution coordinations. Centi et al. [3] and Nilsson et al. [4] have shown that an excess of antimony brings about not only a decrease in activity but also a large increase in the selectivities and in the yields in acrylonitrile and propene. The best catalyst for the synthesis of acrylonitrile from propane has a

---

\*Corresponding author.

large excess of antimony ( $\text{Sb/V}=5.0$ ) [6]. This excess seems to quicken the transformation of the intermediate propene to acrylonitrile. On the contrary, an excess of vanadium brings about not only an increase in activity but also a low selectivity in acrylonitrile due to the increased production of propene and carbon oxides.

The Sn/Sb/O system [7] has been widely studied in recent years as a catalyst active in allylic oxidation and ammoxidation. The best preparation method for these compounds involves coprecipitation from a solution of Sn(IV) and Sb(V) chlorides [8,9]. Calcination at temperatures higher than 700–900°C (depending on the bulk antimony/tin ratio) provokes segregation on the surface of  $\alpha\text{-Sb}_2\text{O}_4$  particles [10]. An antimony surface enrichment, especially for a concentration of antimony lower than 20–30%, [11] and the formation of Sb(III) [9] are evidenced during the thermal treatment. The catalytic activity depends considerably on the Sn/Sb ratio and on the calcination temperature [10,12,13]. In the literature there is also disagreement about the nature of the active sites for allylic oxidation on this system: isolated  $\text{Sb}^{3+}$  species surrounded entirely by  $\text{Sn}^{4+}$  ions in a specific environment [9,10]; an oriented film of  $\text{Sb}_2\text{O}_4$  supported on a solid solution of  $\text{Sb}^{5+}$  in Sn(IV) oxide [8,13]; a solid solution of  $\text{Sb}^{5+}$  ions in a rutile-type matrix [14]; and two “gem”  $\text{Sb}^{5+}=\text{O}$  groups [15].

In order to make a new catalyst for the ammoxidation to acrylonitrile, we decided to mix these two systems: Sb/V, in order to activate the paraffin, and Sn/Sb, which was already utilized to ammoxidate the relative olefin. In this paper, the effects of the atomic ratio of antimony and vanadium and the effects of the method of preparation and calcination of a Sn–V–Sb mixed oxide on its catalytic performance are analyzed. In particular, we changed the amounts of the starting materials and the medium in which the starting materials were dissolved, utilizing ethanol, iso-butanol and water, in order to understand the interaction between the solvent and the metallic ions and to enhance the performance of the catalyst. Moreover, we made a mixture of oxides and hydroxide in *n*-hexane to compare the catalysts prepared by coprecipitation with a simple mixture of the same atomic ratio. The catalyst with the best performance was then calcined at different temperatures and in different atmospheres in order to optimize the thermal treatment.

## 2. Experimental

### 2.1. Catalyst preparation

#### 2.1.1. Coprecipitation method of preparation

Coprecipitation was achieved as follows: initially a solution of anhydrous  $\text{SnCl}_4$  in an organic medium (*absolute ethyl alcohol* or *iso-butanol*) or in an acidic aqueous medium (around HCl 3 M) was prepared; then  $\text{VO}(\text{acac})_2$  and  $\text{SbCl}_5$  were dissolved, in this order, in the solution, in order to obtain the desired Sn/V/Sb ratio. The sequence of the dissolution of the salts is very important in order to obtain a homogeneous solution. The  $\text{VO}(\text{acac})_2$  complex hydrolyzes in a stepwise fashion: hydrolysis of the intermediate  $\text{VO}(\text{acac})^+$  is much slower than the bis-chelate complex at room temperature. When anhydrous  $\text{SnCl}_4$  is dissolved in the organic medium, strongly acid conditions are developed, that are required for the rapid cleavage of both the vanadyl diketonate ligands. This allows complete hydrolysis of the stable  $\text{VO}(\text{acac})_2$ . In addition, the solvolysis effect produced during the dilution of  $\text{SnCl}_4$  in the organic medium further enhances the hydrolysis. This solution was added dropwise to an aqueous solution of  $\text{CH}_3\text{COONH}_4$ , having an initial pH of around 7.0. During the precipitation of the oxohydrates the pH, which decreases due to the release of HCl, was maintained constant by the addition of an ammonia solution. In fact, the pH must not be higher than 7.5 (in order to avoid  $\text{V}^{4+}$  oxidation and to allow precipitation of antimony oxohydrate) and not lower than 5 in order to avoid redissolution of the vanadium and tin oxohydrates. When the precipitation is carried out at a pH outside the mentioned range, there is no simultaneous precipitation of the catalyst components. The resulting precipitate was filtered, washed and dried overnight at 120°C; then calcined at 350°C for 1 h and at 700°C for 3 h.

#### 2.1.2. Solid state reaction preparation

The sample was prepared by a solid state reaction between  $\text{V}_2\text{O}_5$ ,  $\text{Sb}_2\text{O}_3$  and a tin oxohydrate, prepared by precipitating an ethanolic solution of  $\text{SnCl}_4$  in a pH controlled aqueous solution (similar to the previous preparation). The precipitate of  $\text{Sn}(\text{OH})_4$  was filtered, washed and dried at 120°C overnight (drying at

100–140°C leads to the partial dehydration of ortho-stannic acid  $\text{Sn}(\text{OH})_4$  to meta-stannic acid  $\text{SnO}(\text{OH})_4$ . It was then mixed with  $\text{V}_2\text{O}_5$  and  $\text{Sb}_2\text{O}_3$  by suspending the powders in vigorously stirred *n*-hexane. After evaporation of the solvent under reduced pressure, the mixture was dried at 120°C overnight and finally calcined at 350°C for 1 h and at 700°C for 3 h.

The sample with the best performance was re-prepared and, after the drying treatment, was then calcined up to different temperatures in air or in nitrogen in order to study the influence of the thermal treatment.

## 2.2. Characterization

The catalysts were tested in a conventional laboratory apparatus with a tubular fixed bed (length 10 in.; diameter  $\frac{1}{4}$  in.), working at atmospheric pressure and at 360–480°C. The analyses of propane, propene, acrylonitrile, acetonitrile and incondensable gases were made by gas-chromatographic techniques (with Poropack QS and Carbosieve packed columns); ammonia and hydrogen cyanide was detected by absorptions and titrations. The catalytic tests were done with a composition of  $\text{C}_3\text{H}_8:\text{O}_2:\text{N}_2:\text{H}_2:\text{He}=8:20:8:64$  and a contact time of about 3.0 s with the samples of Section 3.1 (relative atomic ratio). For the other catalysts (Section 3.2 method of preparation and Section 3.3 thermal treatment) with a composition of  $\text{C}_3\text{H}_8:\text{O}_2:\text{N}_2:\text{H}_2:\text{He}=25:20:10:45$ , a contact time of 2.0 s was used. The catalyst (2 ml) was loaded as grains (30–40 mesh). A thermocouple, placed in the middle of the catalyst bed, was used to verify that the axial temperature profile was within 3°C.

Surface areas were determined by the BET method with nitrogen absorption at  $-196^\circ\text{C}$  using a Carlo Erba instrument. Fourier transformed infrared (FT-IR) spectra in transmission were recorded using a Perkin-Elmer 7200 Fourier transform spectrometer and KBr disk technique. X-ray diffraction patterns (powder technique) were obtained using Ni-filtered  $\text{Cu K}\alpha$  radiation ( $\lambda=1.542 \text{ \AA}$ ) with a Philips computer controlled instrument (PW1.050/81). XPS analysis was carried out using a Perkin Elmer Model Philips 5500.

## 3. Results and discussion

### 3.1. Effects of the relative atomic ratio

#### 3.1.1. Surface area

The surface areas (Table 1) of all the samples are quite high with respect to the value reported in the literature for the Sn/Sb system. The antimony and vanadium contents in the system seem not to have a unique influence on the surface area of the catalysts.

#### 3.1.2. FT-IR spectroscopy

The spectrum of sample 1 (Sn:V=1.0:0.05), characterized by main bands at 640–680 and 540  $\text{cm}^{-1}$ , connected to the  $\text{SnO}_2$  rutile phase is reported in Fig. 1. The  $\text{SnO}_2$  pure oxide is characterized by three bands at 680, 620 and 520  $\text{cm}^{-1}$  [16]. With the introduction of vanadium, the relative intensities of the three bands change and their wave numbers shift slightly, giving the two bands described before. Moreover, a small band at 988  $\text{cm}^{-1}$  due to the stretching of the  $\text{V}=\text{O}$  double bond is visible. This shifting to lower frequencies with respect to the absorbance of the crystalline  $\text{V}_2\text{O}_5$  (1022  $\text{cm}^{-1}$ ) may be attributed to two effects, firstly to the interactions between the vanadyl species and the rutile-type  $\text{SnO}_2$  matrix and secondly to the electronic effect due to the presence of neighboring reduced vanadium sites.

The presence of antimony in the system again changes the spectra. Only the bands at about 620  $\text{cm}^{-1}$  for the stretching of the  $\text{Sn}-\text{O}$  bond and at 988  $\text{cm}^{-1}$  for the  $\text{V}=\text{O}$  bond are visible (samples 2 and 3). With an excess of antimony (sample 4), in

Table 1  
Atomic ratios and surface areas of samples prepared by coprecipitation

Sample	Medium	Temperature (°C) (atmosphere)	Atomic ratio Sn:V:Sb	Surface area ( $\text{m}^2/\text{g}$ )
1	EtOH	700 (air)	1.0:0.05:0.0	31
2	EtOH	700 (air)	1.0:0.05:0.5	62
3	EtOH	700 (air)	1.0:0.05:1.0	39
4	EtOH	700 (air)	1.0:0.05:2.0	56
5	EtOH	700 (air)	1.0:0.0:1.0	60
6	EtOH	700 (air)	1.0:0.1:1.0	54
7	EtOH	700 (air)	1.0:0.2:1.0	46
8	EtOH	700 (air)	1.0:0.3:1.0	64

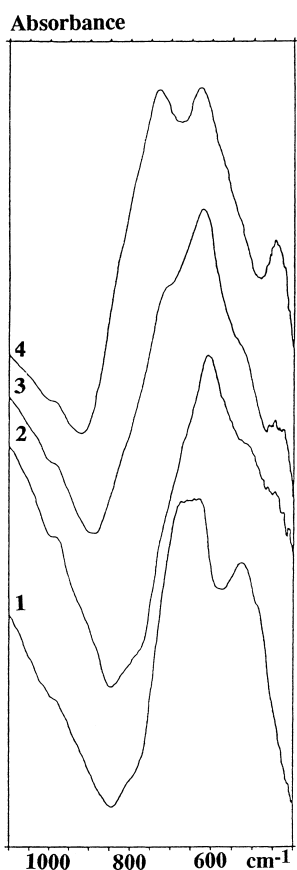


Fig. 1. FT-IR spectra of the samples with increasing amounts of antimony: 1 (Sn:V=1.0:0.05), 2 (Sn:V:Sb=1.0:0.05:0.5), 3 (Sn:V:Sb=1.0:0.05:1.0) and 4 (Sn:V:Sb=1.0:0.05:2.0).

addition to the bands just described, a quite intense band at around  $760\text{ cm}^{-1}$  is also present, typical of the  $\text{Sb}_6\text{O}_{13}$  phase, visible also in the XRD patterns.

The evolution of the infrared spectra with increasing vanadium content is shown in Fig. 2. In this case, modification occurred only for the band at  $988\text{ cm}^{-1}$ . The intensity of this band increases with increasing vanadium content.

### 3.1.3. X-ray diffraction

Reported in Fig. 3 are the X-ray diffractograms of samples with different contents of antimony. Sample 1, without antimony, shows clearly the diffraction lines of the rutile  $\text{SnO}_2$  phase. No other diffraction lines are observed. In the presence of increasing amounts of antimony, the pattern was not modified.

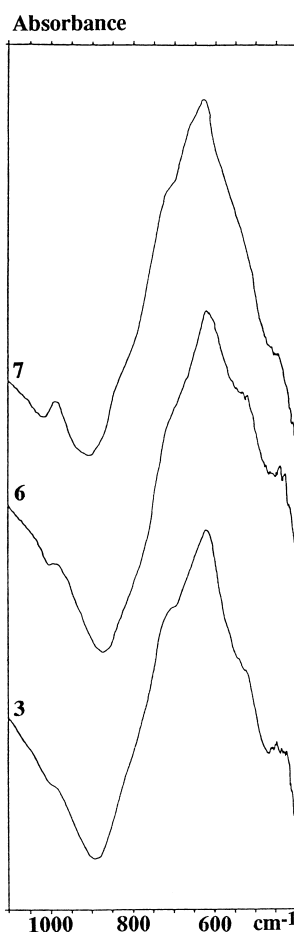


Fig. 2. FT-IR spectra of the samples with increasing amounts of vanadium: 3 (Sn:V:Sb=1.0:0.05:1.0), 6 (Sn:V:Sb=1.0:0.1:1.0) and 7 (Sn:V:Sb=1.0:0.2:1.0).

Only for sample 4 (Sn:V:Sb=1.0:0.05:2.0) did the diffraction lines typical of crystalline  $\text{Sb}_6\text{O}_{13}$  appear. Thus, antimony oxide, if present in the other samples, was completely amorphous.

Samples containing Sn:Sb=1:1 and different amounts of V (Fig. 4) exhibit the same pattern relative to the rutile phase. In the presence of increasing amounts of vanadia, the pattern is not modified.

In each figure and especially in Fig. 3, with increasing antimony content, a shift of the reflection to higher  $2\theta$  values is observed. In order to evidence the interactions between the  $\text{SnO}_2$  matrix with the antimony and the vanadium, the  $a$  and  $c$  parameter of the  $\text{SnO}_2$  tetragonal cell (Tables 2 and 3) were measured. These

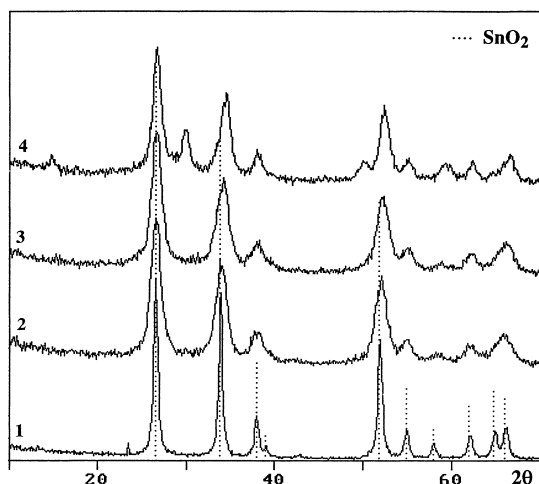


Fig. 3. XRD patterns of the samples with increasing amounts of antimony: 1 (Sn:V=1.0:0.05), 2 (Sn:V:Sb=1.0:0.05:0.5), 3 (Sn:V:Sb=1.0:0.05:1.0) and 4 (Sn:V:Sb=1.0:0.05:2.0).

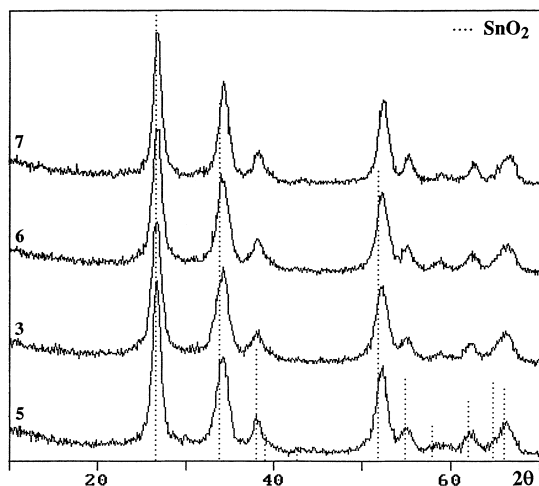


Fig. 4. XRD patterns of the samples with increasing amounts of vanadium: 5 (Sn:Sb=1.0:1.0), 3 (Sn:V:Sb=1.0:0.05:1.0), 6 (Sn:V:Sb=1.0:0.1:1.0) and 7 (Sn:V:Sb=1.0:0.2:1.0).

parameters decrease as the content of antimony in the samples increases, showing a cell contraction due to the substitution of  $\text{Sn}^{4+}$  with smaller ions. In particular, owing to the dimension of the ions in solution ( $\text{Sn}^{4+}=0.71$ ,  $\text{Sb}^{3+}=0.76$ ,  $\text{Sb}^{5+}=0.62$  Å), it is possible to hypothesize the introduction of  $\text{Sb}^{5+}$  inside the rutile structure, in substitutional solid solution. The trend of the cell parameters with the vanadium content

Table 2

Cell parameters and volume of the samples with increasing amounts of antimony

Sample	Composition	<i>a</i> (Å)	<i>c</i> (Å)	<i>V</i> (Å <sup>3</sup> )
1	Sn:V:Sb=1.0:0.05:0.0	4.727	3.177	70.99
2	Sn:V:Sb=1.0:0.05:0.5	4.724	3.151	70.31
3	Sn:V:Sb=1.0:0.05:1.0	4.712	3.147	69.87
4	Sn:V:Sb=1.0:0.05:2.0	4.715	3.114	69.22

Table 3

Cell parameters and volume of the samples with increasing amounts of vanadium

Sample	Composition	<i>a</i> (Å)	<i>c</i> (Å)	<i>V</i> (Å <sup>3</sup> )
5	Sn:V:Sb=1.0:0.0:1.0	4.720	3.134	69.82
3	Sn:V:Sb=1.0:0.05:1.0	4.712	3.147	69.89
6	Sn:V:Sb=1.0:0.1:1.0	4.705	3.145	69.62
7	Sn:V:Sb=1.0:0.2:1.0	4.702	3.136	69.33

is more complex. Meanwhile the introduction of vanadium in the  $\text{SnO}_2$  rutile-type structure [16] has evidenced a solubility limit directly related to the trend of the cell parameters. In this case the presence of antimony modifies the system considerably. Nevertheless, the increase in vanadium content modifies the volume of the rutile-type cell, indicating the substitution of tin with smaller ions.

### 3.1.4. Catalytic tests

The catalytic performance in propane ammoxidation of the sample containing increasing amounts of antimony and vanadium is reported in Figs. 5–8.

It is possible to see that, as the amount of antimony increases (samples 2–4), the activity decreases considerably (Fig. 5), but the selectivity (Fig. 6) and maximum yield of acrylonitrile increase. On the contrary, quantities of antimony higher than these values do not bring about great improvements in the acrylonitrile yields. In fact the higher selectivity is counter balanced by a very low activity (and the too high reaction temperature leads to total combustion).

The activity of sample 3 is quite good, reaching 30% of conversion at about 510°C. Nevertheless, even if the acrylonitrile selectivities reached with this sample are interesting (i.e.  $S_{\text{ACN}}=40\%$  at  $C=20\%$ ), working at temperatures around 500°C has the opposite effect, i.e. enhancing the production of carbon oxides,

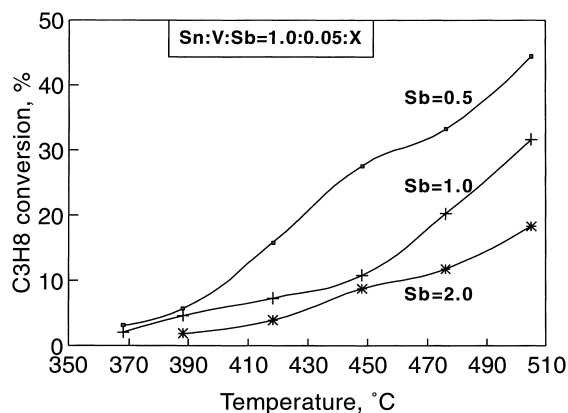


Fig. 5. Propane conversion vs. reaction temperature for the samples with increasing amounts of antimony: 2 (Sn:V:Sb=1.0:0.05:0.5), 3 (Sn:V:Sb=1.0:0.05:1.0) and 4 (Sn:V:Sb=1.0:0.05:2.0).

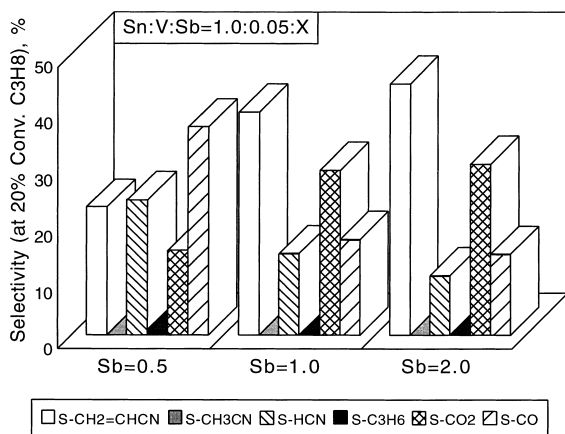


Fig. 6. Selectivity at conversion of 20% for the samples with increasing amounts of antimony: 2 (Sn:V:Sb=1.0:0.05:0.5), 3 (Sn:V:Sb=1.0:0.05:1.0) and 4 (Sn:V:Sb=1.0:0.05:2.0).

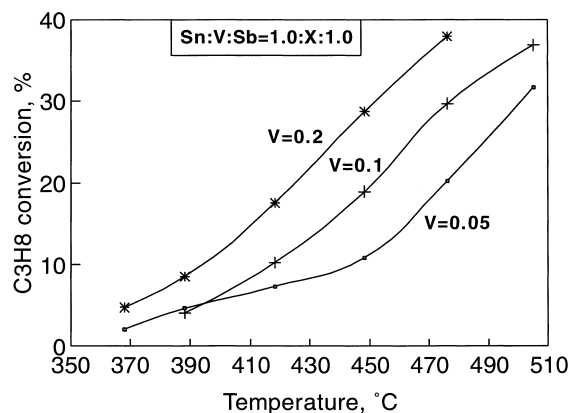


Fig. 7. Propane conversion vs. reaction temperature for the samples with increasing amounts of vanadium: 3 (Sn:V:Sb=1.0:0.05:1.0), 6 (Sn:V:Sb=1.0:0.1:1.0) and 7 (Sn:V:Sb=1.0:0.2:1.0).

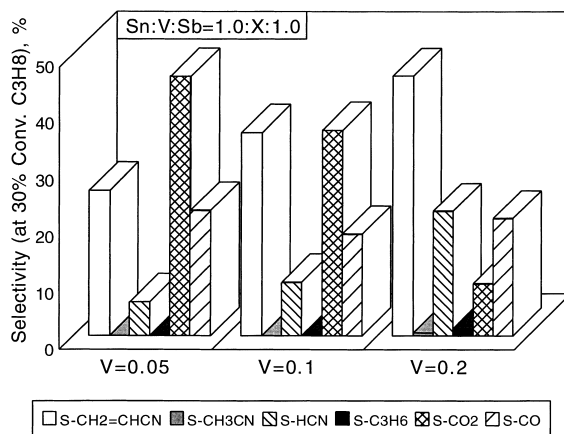


Fig. 8. Selectivity at conversion of 30% for the samples with increasing amounts of vanadium: 3 (Sn:V:Sb=1.0:0.05:1.0), 6 (Sn:V:Sb=1.0:0.1:1.0) and 7 (Sn:V:Sb=1.0:0.2:1.0).

also by the consecutive reaction of combusting the desired product. In order to minimize this effect and to enhance the activity without decreasing too much the acrylonitrile selectivity, we decided to increase the amount of vanadium (keeping constant the amount of antimony) in sample 3. Samples 6–8 were prepared, which contain, respectively, twice, four and six times the amount of vanadium in sample 3.

Reported in Figs. 7 and 8 are conversion vs. reaction temperature and the selectivities at iso-conversion (30%) for the samples with increasing vanadium

content. It is possible to see that the vanadium creates sites which increase the activity of the sample (Fig. 7). Moreover, due to the low reaction temperature utilized to reach the same conversion, the sample with a higher content of vanadium shows also an increase in the acrylonitrile selectivity. In other words, the influence of the vanadium on the catalytic performance of this system is to enhance the activity, shifting the conversion line to lower temperatures. In this way it is possible to obtain high conversion at a lower temperature, minimizing the undesired consecutive reaction of

combustion. Hence the quantity of the desired product is enhanced. In fact if we compare the acrylonitrile selectivity at low conversion, the samples are similar; but at higher conversion, with low vanadium content, the acrylonitrile selectivity is low, due to high carbon oxides selectivity. Sample 8 with the highest vanadium content ( $V/Sn=0.3$ ) shows considerable activity, but a very low acrylonitrile selectivity. The ratio  $V/Sn=0.2$  seems to be the stabilization limit of vanadium in the system. Higher amounts of vanadium are not sufficiently dispersed in the catalyst matrix, leading to combustion.

The present data indicate some interesting aspects of the catalytic chemistry of  $Sn/V/Sb$  mixed oxides. In fact, the results show that the  $Sn/V$  matrix is responsible for the activation of propane, meanwhile antimony has mainly the function of moderating the oxidative property of the system, permitting nitrogen insertion in the molecule (in other words it can be considered as an acrylonitrile selectivity modulator). The sample with the best performance is sample 7 with the ratio  $Sn:V:Sb=1:0.2:1$ , that reaches conversion of 40% and acrylonitrile selectivity higher than 40% in the experimental conditions employed.

### 3.2. Effects of the preparation method

On the basis of the results obtained, another three catalysts with the same atomic ratio of sample 7 ( $Sn:V:Sb=1.0:0.2:1.0$ ), but prepared with different methods, were synthesized (Table 4).

#### 3.2.1. Surface area

The surface areas of the four samples are reported in Table 4. The catalysts have a similar value of surface area; the one prepared from oxides and tin hydroxide (sample 11) shows the lowest value.

Table 4

Surface areas of samples having the same atomic ratio as samples 7, but prepared with different methods

Sample	Medium	Temperature (°C) (atmosphere)	Atomic ratio $Sn:V:Sb$	Surface area ( $m^2/g$ )
7	EtOH	700 (air)	1.0:0.2:1.0	46
9	H <sub>2</sub> O	700 (air)	1.0:0.2:1.0	54
10	<i>i</i> -BuOH	700 (air)	1.0:0.2:1.0	62
11	<i>n</i> -Hexane	700 (air)	1.0:0.2:1.0	32

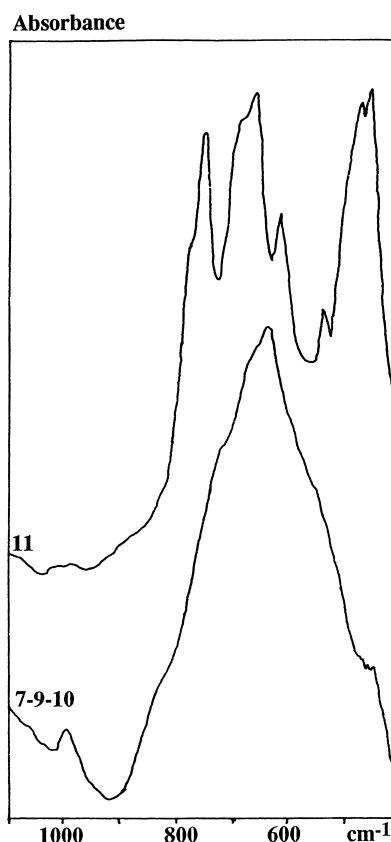


Fig. 9. FT-IR spectra of the samples prepared with different techniques: 7, 9, 10 (coprecipitation) and 11 (solid state reaction).

#### 3.2.2. FT-IR spectroscopy

FT-IR spectra of the four samples are reported in Fig. 9. The catalysts prepared by coprecipitation (7, 9 and 10) have the same FT-IR spectra. It is possible to see the stretching absorbance of the  $V=O$  bond at around  $988\text{ cm}^{-1}$  and of the  $Sn-O$  bond at  $620\text{ cm}^{-1}$  described in Section 3.1.2. The spectra of sample 11, prepared using a mixture of  $V$  and  $Sb$  oxides and  $Sn$  hydroxide in hexane, is very different from the others. It shows the absorbance bands of  $\alpha\text{-Sb}_2\text{O}_4$  at 745, 648, 605 and  $529\text{ cm}^{-1}$  and a weak band at  $1020\text{ cm}^{-1}$ , typical of crystalline  $V_2O_5$ .

#### 3.2.3. X-ray diffraction

The diffractograms of these four samples are reported in Fig. 10. The samples prepared by coprecipitation are very similar and show clearly the dif-

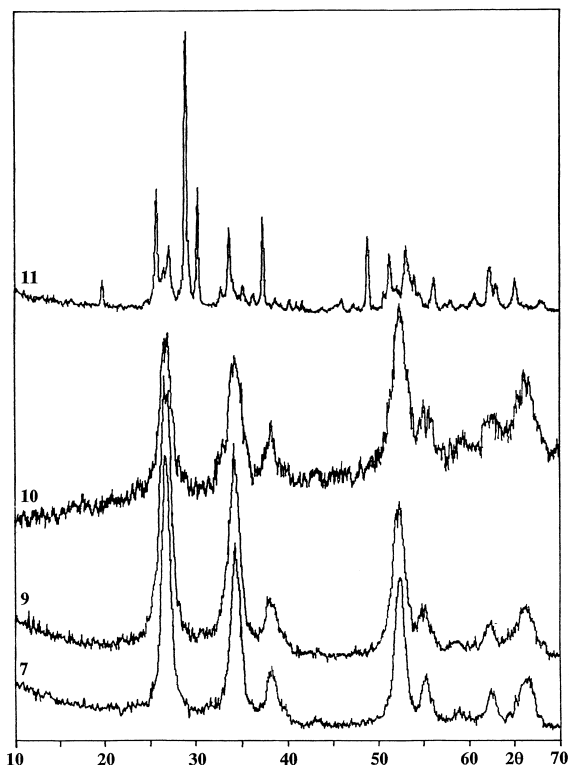


Fig. 10. XRD patterns of the samples prepared with different solvents: 7 (ethanol), 9 (water), 10 (iso-butanol) and 11 (solid state reaction).

fraction lines of the rutile-type  $\text{SnO}_2$  phase. The reflections are very broad, due to the very small crystallites and no other phases are present. It should be noted however that, due to the broadness of the diffraction lines of  $\text{SnO}_2$ , the possible presence of the rutile-type  $\text{VSbO}_4$  phase would be difficult to evidence. When the preparation is carried out by solid state reaction (sample 11), the XRD patterns change drastically, as was also observed in the FT-IR characterization. The main phase present is  $\alpha\text{-Sb}_2\text{O}_4$ , moreover, the weak peaks of  $\text{SnO}_2$  are also present.

### 3.2.4. Catalytic tests

Reported in Figs. 11 and 12 are conversion vs. temperature and acrylonitrile selectivity vs. conversion, respectively, for these four samples. Even if the catalysts reach similar conversions, they have different activities, due to their different working temperature

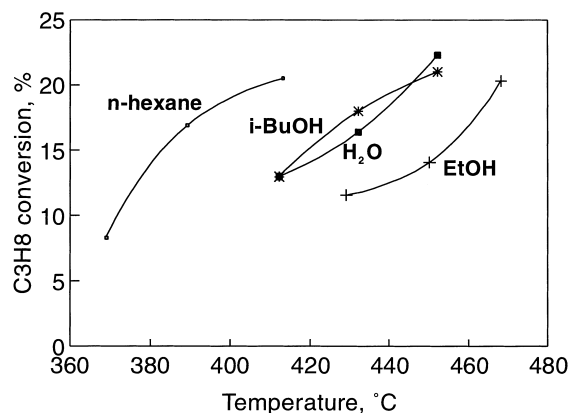


Fig. 11. Propane conversion vs. reaction temperature for the samples prepared with different solvents: 7 (ethanol), 9 (water), 10 (iso-butanol) and 11 (solid state reaction).

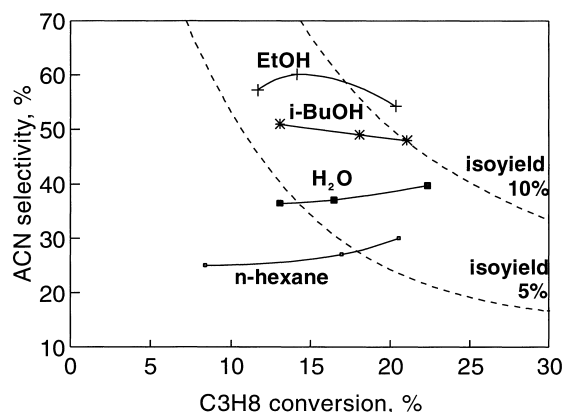


Fig. 12. Acrylonitrile selectivity vs. propane conversion for the samples prepared with different solvents: 7 (ethanol), 9 (water), 10 (iso-butanol) and 11 (solid state reaction).

range. The acrylonitrile selectivity is very different. Sample 7 (EtOH) is the best one, reaching a value of 60%, then the order decreases as follows: sample 10 (*i*-BuOH), sample 9 (water) and sample 11 (*n*-hexane). Hence, while the catalytic data of the samples prepared by the coprecipitation technique are different, the structural characterization did not reveal meaningful differences. The use of ethanol as the solvent for dissolution of the ions brings about the partial formation of tin-, antimony- and vanadyl-alkoxide, which slows down the precipitation of the different compounds, making their respective velocities uniform. In



this way a better interaction among the hydroxides is achieved and the better dispersion of the active sites brings about the necessary multifunctionality to convert a saturated hydrocarbon into a functionalized molecule with good selectivity. The alkoxides are more difficult to obtain with a sterically hindered alcohol such as iso-butanol and similar equilibria do not exist with water. Hence, by using water or iso-butanol as the solvent, the precipitation velocities of the different compounds can be different, leading to poor dispersion of the active sites, which in turn means low acrylonitrile selectivity. The solid state reaction method of preparation (sample 11) leads to a mixture of oxides and not to a mixed oxide. Indeed the characterization techniques used showed a segregation of the system into the single oxides. Consequently the mixture of the active sites is not good and the acrylonitrile selectivity falls considerably.

### 3.3. Effects of the thermal treatment

Sample 7 (ethanol) was re-prepared and calcined at 500°C, 700°C and 800°C in air and in nitrogen, as reported in Table 5.

#### 3.3.1. Surface area

The surface areas of the samples calcined at different temperatures, both in air and in nitrogen are summarized in Table 5. The surface area decreases as calcination temperature increases due to the destruction of the microporosity. Moreover, the sample calcined in air has a higher surface area than the one calcined at the same temperature in nitrogen.

Table 5

Surface areas of samples with the same composition and preparation method as sample 7, but calcined with different thermal treatments

Sample	Medium	Temperature (°C) (atmosphere)	Atomic ratio Sn:V:Sb	Surface area (m <sup>2</sup> /g)
12	EtOH	500 (air)	1.0:0.2:1.0	114
7	EtOH	700 (air)	1.0:0.2:1.0	46
13	EtOH	800 (air)	1.0:0.2:1.0	32
14	EtOH	500 (nitrogen)	1.0:0.2:1.0	74
15	EtOH	700 (nitrogen)	1.0:0.2:1.0	26
16	EtOH	800 (nitrogen)	1.0:0.2:1.0	18

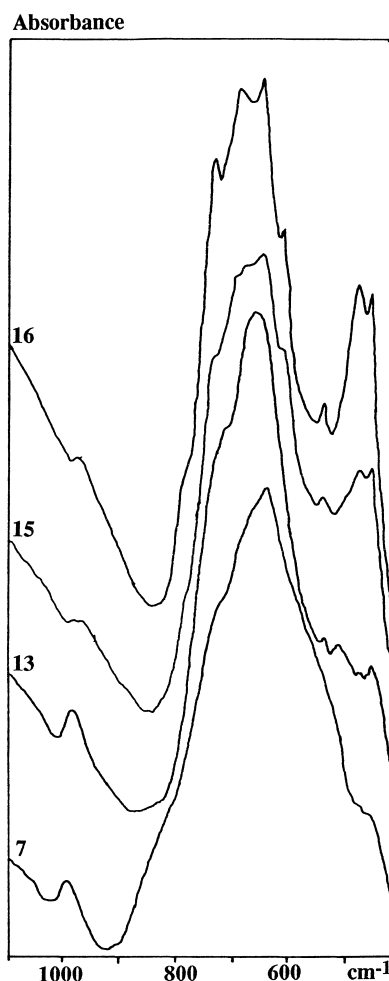


Fig. 13. FT-IR spectra of the samples calcined with different thermal treatments: 7 (700°C in air), 13 (800°C in air), 15 (700°C in nitrogen) and 16 (800°C in nitrogen).

#### 3.3.2. FT-IR spectroscopy

The FT-IR spectra of samples calcined at high temperatures (7, 13, 15 and 16), both in air and in nitrogen are shown in Fig. 13.

The FT-IR spectra of the samples calcined in air are quite similar, with the typical absorbance bands of tin oxide (around 629 cm<sup>-1</sup>) and vanadyl species (around 988 cm<sup>-1</sup>) described in Section 3.2. After treatment at higher temperatures, with an increase in crystallinity and the progressive evolution of volatile compounds, the band, typical of the Sn–O bond in the Sn/Sb system, becomes more well-defined. Moreover, some initial modifications of the spectra due to the Sb–O–Sb

bond of antimony oxides are observed in the sample calcined at 800°C.

The band typical of vanadyl species is much less intense in the spectra of samples calcined in nitrogen. Moreover, in a nitrogen atmosphere, the typical bonds of antimony oxides are observed, even after treatment at 700°C, indicating greater segregation of the different phases during calcination in the inert gas. Hence, the evolution of phases with temperature, as evidenced using FT-IR, depends considerably on the calcination atmosphere.

### 3.3.3. X-ray diffraction

XRD data for the samples calcined in air at 700°C and 800°C and in nitrogen at 700°C (7, 13 and 15) are reported in Fig. 14.

The diffractogram for sample 7 calcined at 700°C in air shows only the reflections of the rutile-type  $\text{SnO}_2$  and the diffractogram of the sample calcined in air at

500°C is similar, even if less crystalline. Moreover, due to the broadness of the diffraction lines, the possible presence of the rutile  $\text{VSbO}_4$  phase would be difficult to observe. On the contrary, the diffractogram of the sample calcined in air at 800°C is very different. Both  $\text{SnO}_2$  and  $\text{Sb}_2\text{O}_4$  phases ( $\beta\text{-Sb}_2\text{O}_4$  and  $\alpha\text{-Sb}_2\text{O}_4$ ) are present and the crystallinity of the samples is greater, as evidenced by the narrowing of the diffraction lines and lowering of the background signal, for the samples obtained at 800°C. The formation of  $\beta\text{-Sb}_2\text{O}_4$  under these conditions was not expected, since direct oxidation of antimony oxide produces  $\alpha\text{-Sb}_2\text{O}_4$ , which is converted to  $\beta\text{-Sb}_2\text{O}_4$  at 1130°C. Berry [9] proposed that the  $\beta\text{-Sb}_2\text{O}_4$  phase obtained during the preparation of the  $\text{VSbO}_4$  phase was more accurately described as a solid solution of vanadium in  $\beta\text{-Sb}_2\text{O}_4$  and that the vanadium facilitates and stabilizes the low temperature formation of this phase. Thus, also in our case, the formation of  $\beta\text{-Sb}_2\text{O}_4$  at low temperature can be favored by the migration of some vanadium ions to form a solid solution within this phase.

In spite of the high content of Sb in the catalyst, the X-ray diffraction patterns up to 700°C show only the lines due to rutile-type  $\text{SnO}_2$ . No lines due to antimony oxides are observed, but the diffraction lines of the rutile phase in all the Sn/V/Sb samples are shifted towards lower  $d$  values with respect to those of pure  $\text{SnO}_2$ . This observation can be attributed to the substitution of Sb and/or V ions in the tin(IV) oxide lattice. Table 6 shows the rutile tetragonal cell volume for samples calcined at different temperatures in air. In these samples the cell volume increases, with increasing calcination temperature, reaching values closer to (but still lower than) that of pure  $\text{SnO}_2$ . This behavior indicates a substitution of  $\text{Sn}^{4+}$  by ions with an atomic radius lower than 0.69 Å ( $\text{V}^{3+}=0.64$ ;  $\text{V}^{4+}=0.58$ ;

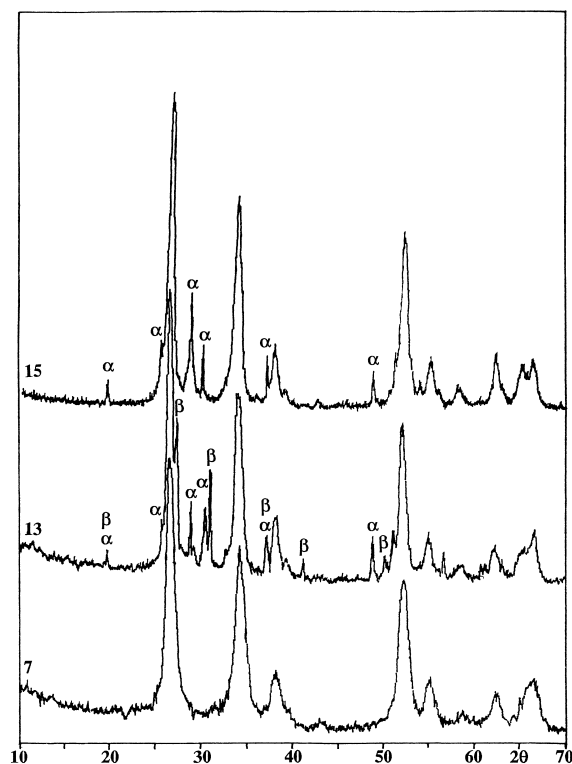


Fig. 14. XRD patterns of the samples calcined with different thermal treatments: 7 (700°C in air), 13 (800°C in air) and 15 (700°C in nitrogen).

Table 6

Cell parameters and volume of rutile  $\text{SnO}_2$  of the samples calcined in air and in nitrogen

Sample	Thermal treatment	$a$ (Å)	$c$ (Å)	$V$ (Å <sup>3</sup> )
7	700°C (air)	4.70	3.14	69.36
13	800°C (air)	4.70	3.16	69.83
15	700°C (nitrogen)	4.70	3.18	70.24
16	800°C (nitrogen)	4.70	3.17	69.97
Pure $\text{SnO}_2$	—	4.74	3.19	71.55

$V^{5+}=0.54$ ;  $Sb^{3+}=0.76$ ;  $Sb^{5+}=0.60$  Å), this substitution should be higher at lower temperatures and it seems to decrease with increasing calcination temperature. Moreover, since it is known that an antimony concentration as low as 5–6% may represent the upper limit of antimony incorporation in the tin(IV) oxide lattice [9], it is probable that the excess antimony can be present as an amorphous phase together with the doped rutile structure.

Also reported in Fig. 14 is the diffractogram of sample 15 calcined in nitrogen at 700°C. The diffractogram of a sample calcined at 600°C shows the  $SnO_2$  phase only (like sample calcined in air at 700°C); on the contrary, in a nitrogen atmosphere, the formation of crystalline antimony oxides shifts to a lower temperature with respect to that in air (700°C instead of 800°C) and the main phase evidenced, besides  $SnO_2$ , is only  $\alpha$ - $Sb_2O_4$  and not  $\beta$ - $Sb_2O_4$ .

Table 6 shows the effect of the calcination temperature in nitrogen on the crystallographic parameters. Also in this case, the cell volume of the Sn/V/Sb system is lower than pure  $SnO_2$ , but the values are different from samples calcined in air, evidencing a different extent of substitution in the rutile structure. Since the cell volume obtained by calcination in air is lower, we can hypothesize that, during calcination in nitrogen, lower amounts of antimony and vanadium ions enter the rutile structure to form a solid solution; thus, the presence of oxygen during calcination seems to favor the formation of a solid solution.

### 3.3.4. X-ray photoelectron spectroscopy

The materials, calcined at different temperatures and under different atmospheres were studied by XPS analysis in order to determine the surface composition and the oxidation state of tin, vanadium and antimony in each of the samples. Table 7 reports the atomic percentage of tin, vanadium and antimony in the various catalysts. The bulk atomic ratio analysis was made by atomic absorption and the surface atomic ratio by XPS spectroscopy.

The results show that the surface vanadium content in catalysts calcined in air is quite close to the bulk composition. Moreover, the  $V_{XPS}$  intensity remains almost constant with increasing calcination temperature. On the contrary, the Sb surface composition is similar to the bulk composition only at low temperatures and we observed an enhancement of the signal up

Table 7

Bulk and surface relative atomic ratio of the samples calcined in different conditions

Sample	Thermal treatment	Atomic ratio Sn:V:Sb	
		Bulk	Surface
12	500°C (air)	5.0:1.0:4.9	5.0:1.0:4.8
7	700°C (air)	5.0:1.0:4.9	5.0:1.2:5.9
13	800°C (air)	5.0:1.0:4.9	5.0:1.2:3.7
14	500°C (nitrogen)	5.0:1.0:4.8	5.0:0.8:4.7
15	700°C (nitrogen)	5.0:1.0:4.8	5.0:0.8:4.5

to 700°C and a decrease after calcination at 800°C in air. This last phenomena can be due to: (i) migration of antimony into the rutile structure and (ii) aggregation of antimony particles. The latter is more acceptable because XRD analysis of the sample calcined at 800°C in air shows the segregation of the  $Sb_2O_4$  phase. In a nitrogen environment a much less pronounced effect of temperature is observed, but the vanadium surface composition of these samples is lower than in the bulk, indicating a probable aggregation of vanadium particles.

XPS analysis was also utilized to estimate the oxidation state of the different elements present in the system. Table 8 shows the degree of oxidation for vanadium and antimony ions; the oxidation state of tin is always  $Sn^{4+}$ .

The XPS analysis showed the presence of  $Sb^{3+}$ ,  $Sb^{5+}$ ,  $V^{4+}$  and  $V^{5+}$  species in oxidizing environments. In all the samples, the surface antimony is mainly present as  $Sb^{5+}$  and the maximum content of  $Sb^{3+}$  is 5%. The surface vanadium is present both as  $V^{5+}$  and  $V^{4+}$  and the amount of  $V^{4+}$  present on air calcined

Table 8

Estimation of relative amounts of antimony and vanadium in the Sn/V/Sb system

Sample	Thermal treatment	Atomic percentage (%)			
		Antimony 3d 5/2		Vanadium 2p	
		$Sb^{3+}$	$Sb^{5+}$	$V^{4+}$	$V^{5+}$
12	500°C (air)	4	96	33	67
7	700°C (air)	5	95	39	61
13	800°C (air)	5	95	44	56
14	500°C (nitrogen)	2	98	51	49
15	700°C (nitrogen)	3	97	51	49

samples increases with increasing calcination temperature. This behavior can be due to the formation of a stable structure containing  $V^{4+}$  even though the content of surface vanadium measured by XPS did not show any decrease due to segregation of the new phase. On the contrary, the  $V_{XPS}$  signals of samples calcined at different temperatures in nitrogen remain unchanged and show a higher degree of reduction of these samples with respect to the samples calcined in air.

### 3.3.5. Catalytic tests

Reported in Figs. 15 and 16 are conversion vs. temperature and acrylonitrile selectivity vs. conversion, respectively, for the six samples calcined at different temperatures, both in air and in nitrogen. By comparing these data with the structural characterization reported before, the following conclusions can be made.

The activity of samples 12 and 14 calcined at 500°C is quite high, but the selectivity in acrylonitrile is very low, owing to combustion. The high surface area of the sample calcined at low temperature negatively influences the catalytic performance.

Sample 13 calcined in air at 800°C is less selective in acrylonitrile with respect to sample 7 calcined at 700°C. This decrease is caused by the structural evolution of the system with segregation of the antimony oxide.

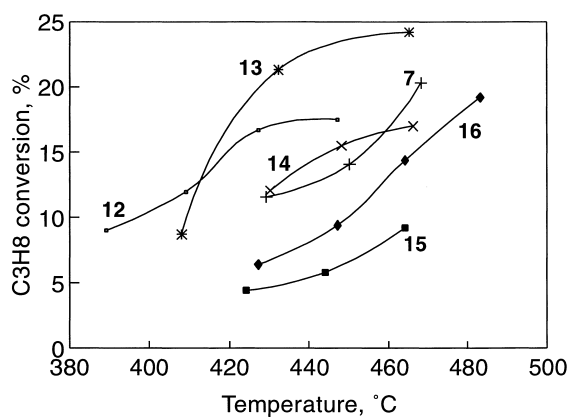


Fig. 15. Propane conversion vs. reaction temperature for the samples calcined with different thermal treatments: 12 (500°C in air), 7 (700°C in air), 13 (800°C in air), 14 (500°C in nitrogen), 15 (700°C in nitrogen) and 16 (800°C in nitrogen).

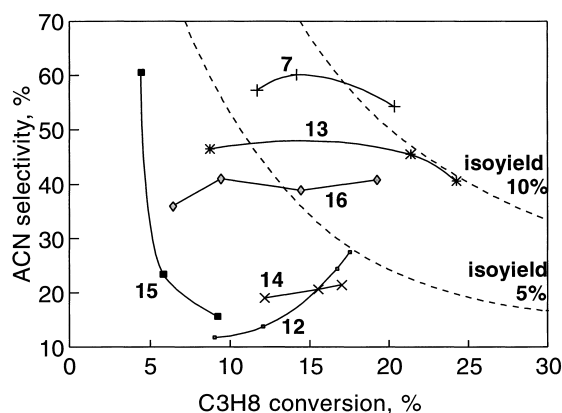


Fig. 16. Acrylonitrile selectivity vs. propane conversion for the samples calcined with different thermal treatments: 12 (500°C in air), 7 (700°C in air), 13 (800°C in air), 14 (500°C in nitrogen), 15 (700°C in nitrogen) and 16 (800°C in nitrogen).

Sample 15 calcined in nitrogen at 700°C is less active with respect to sample 7 calcined in air at the same temperature and the selectivity in acrylonitrile is very low, owing to combustion. The absence of vanadyl species, evidenced by FT-IR spectra, seems to influence the catalytic performance of the mixed oxide in a dramatically negative way.

When the temperature of calcination in a nitrogen atmosphere increased (from 700°C to 800°C), the sample becomes more active and selective in acrylonitrile, but still less than that of the catalyst calcined in air at 700°C. The presence of different phases and of a non-homogeneously distributed mixed oxide leads to a less selective sample for propane ammoxidation.

## 4. Conclusions

The general conclusion that can be drawn from this work is that our original method of preparation using a coprecipitation procedure from the ethanolic phase [17] leads to a more intimate mixture of tin, antimony and vanadium, inducing a spreading of the active component that promotes active site isolation [18] and stabilizes the active phase. During the thermal treatment the catalytic system evolves from a homogeneous mixed oxide, where numerous well-crystallized microfields of  $SnO_2$  incorporating antimony and vanadium ions in a limited concentration are dispersed

in an excess of poorly crystallized  $\text{SbO}_x$ , to a mixture of antimony oxide and rutile-type solid solution. In fact, when the calcination temperature is increased up to 800°C (in air) or 700°C (in nitrogen) the antimony ions migrate forming a segregated antimony oxide. The catalytic performance for the ammoxidation of propane appears to be related to an enhanced antimony content in the surface (evidenced by XPS analysis) in poorly crystalline materials, i.e. samples in which the antimony in excess is highly dispersed and amorphous. High calcination temperatures cause the migration and phase segregation of antimony to the surface and a corresponding decrease in the selectivity to acrylonitrile formation.

## References

- [1] G. Centi, R.K. Grasselli, F. Trifirò, *Catal. Today* 13 (1992) 661.
- [2] G. Centi, D. Pesheva, F. Trifirò, *Appl. Catal.* 33 (1987) 343.
- [3] G. Centi, F. Trifirò, R.K. Grasselli, *La Chimica and L'Industria* (Milan) 72 (1990) 617.
- [4] R. Nilsson, T. Lindblad, A. Andersson, C. Song, S. Hansen, in: V. Cortes Corberan, S. Vic Bellon (Eds.), *New Developments in Selective Oxidation II*, *Stud. Surf. Sci. Catal.* 82 (1994) 293.
- [5] G. Centi, R.K. Grasselli, E. Patanè, F. Trifirò, in: G. Centi, F. Trifirò (Eds.), *New Developments in Selective Oxidation*, *Stud. Surf. Sci. Catal.* 55 (1990) 515.
- [6] A.T. Guttman, R.K. Grasselli, J.F. Bradzil, D.D. Suresh, US Patent 4 746 641 (1988), assigned to The Standard Oil Co.
- [7] G. Centi, F. Trifirò, *Catal. Rev.-Sci. Eng.* 28 (1986) 165.
- [8] J.C. Volta, P. Bussiere, G. Coudurier, J.M. Herrmann, J.C. Vedrine, *Proceedings of the IX Ibero-American Symposium on Catalysis*, Lisbon, 1984, p. 888.
- [9] F.J. Berry, *Adv. Catal.* 30 (1981) 97.
- [10] H.J. Hermiman, D.R. Pyke, R. Reid, *J. Catal.* 58 (1979) 68.
- [11] Y.M. Cross, D.R. Pyke, *J. Catal.* 58 (1979) 61.
- [12] F. Trifirò, I. Pasquon, *La Chimica and L'Industria* (Milan) 52 (1970) 228.
- [13] Y. Boudeville, F. Figueras, M. Forissier, J.L. Portefaix, J.C. Vedrine, *J. Catal.* 58 (1979) 52.
- [14] G.M. Godin, C.C. McCain, E.A. Porter, *Proceedings of the Fourth International Congress on Catalysis*, vol. 1, Akademiai Kiado, Budapest, 1971, p. 271.
- [15] F. Sala, F. Trifirò, *J. Catal.* 41 (1976) 1.
- [16] S. Bordoni, F. Castellani, F. Cavani, F. Trifirò, M. Gazzano, *J. Chem. Soc., Faraday Trans.* 90 (1994) 2981.
- [17] S. Albonetti, G. Blanchard, P. Burattin, F. Cavani, F. Trifirò, France Patent 94-07982-1994, assigned to Rhone Poulenc Chimie.
- [18] J.L. Callahan, R.K. Grasselli, *AIChE J.* 9 (1963) 755.